Supplementary Materials for

The Advent of Membrane-Less Zinc-Anode Aqueous Batteries with Lithium-like Voltage

Gautam G. Yadav[1]*, Meir Weiner[1], Aditya Upreti[1], Jinchao Huang[1], Timothy N. Lambert[3], David J. Arnot[3], Noah B. Schorr[3], Nelson S. Bell[3], Damon Turney[2], Brendan Hawkins[2], Xia Wei[2], Matthew Lim[3] and Sanjoy Banerjee[2]

[1]Research and Development Department, Urban Electric Power, 401 N. Middletown Road, Pearl River, New York, 10965

[2]The CUNY Energy Institute at the City College of New York, Department of Chemical Engineering, Steinman Hall Rm 316, 160 Convent Ave. New York, 10031, USA

[3]Sandia National Laboratories, Albuquerque, New Mexico 87185

Correspondence to: Gautam G. Yadav (gautam@urbanelectricpower.com)

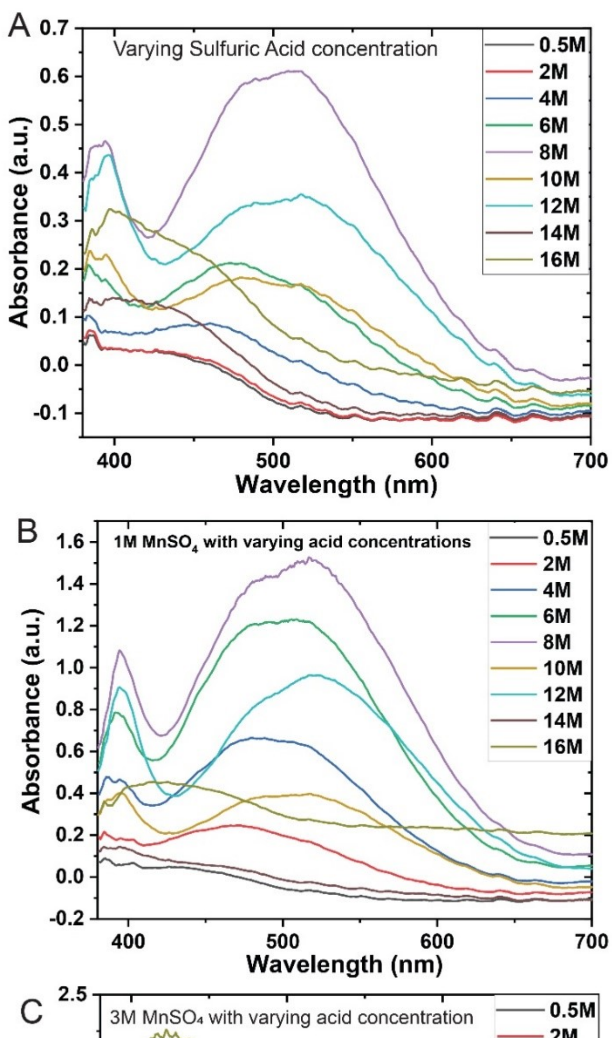

Supplementary Figure 1. (A) UV-vis spectra of catholyte solutions with varying acid concentrations. (B) UV-vis spectra of catholyte solutions with varying acid concentrations containing 1M manganese sulfate. (C) UV-vis spectra of catholyte solutions with varying acid concentrations containing 3M manganese sulfate.

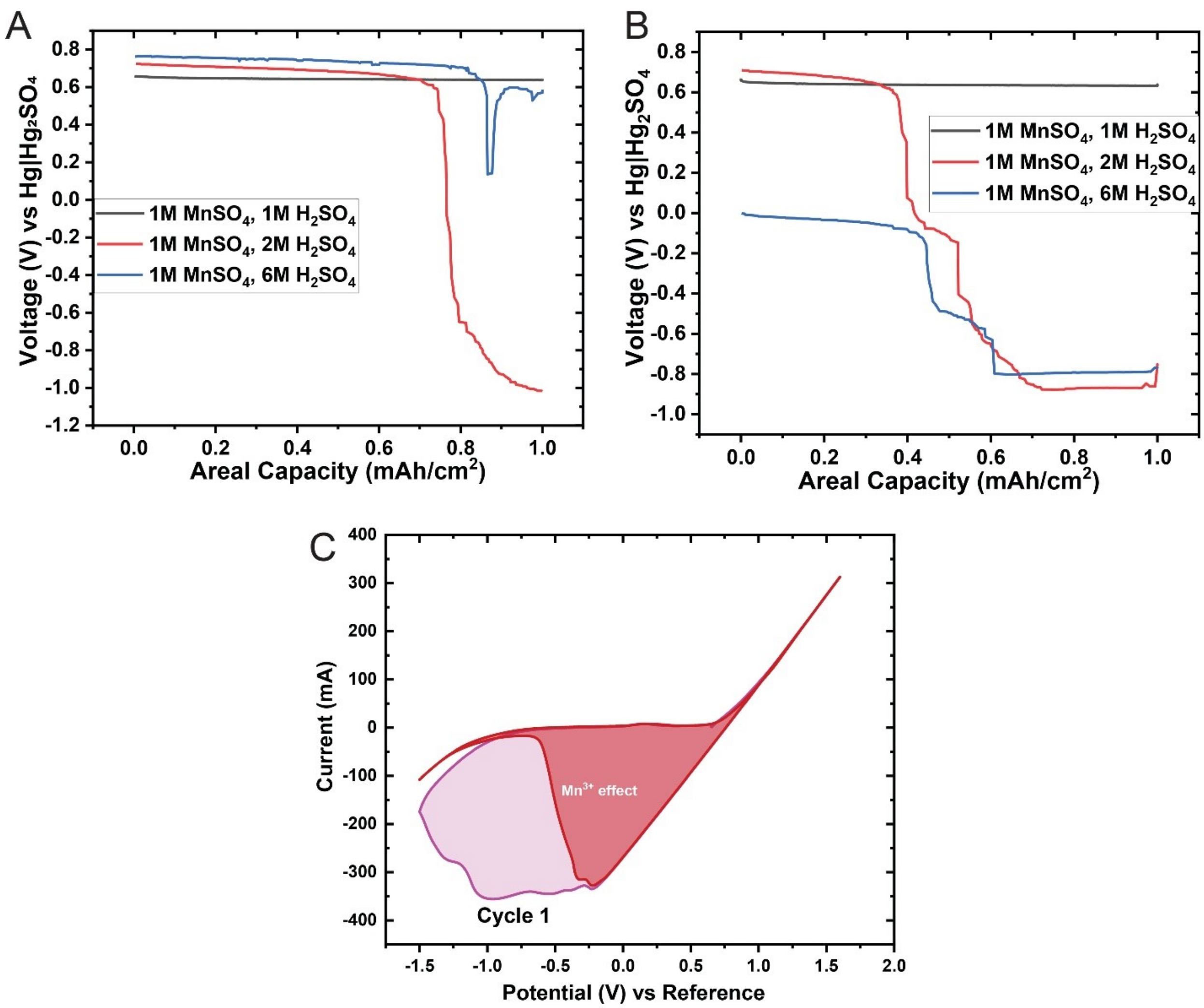

Supplementary Figure 2. (A) Initial discharge capacity curves of MnO_2 in 1M $MnSO_4$ with varying acid concentrations. (B) Discharge capacity curves in later cycles for MnO_2 in 1M $MnSO_4$ with varying acid concentrations. (C) Cyclic voltammetry data of MnO_2 showing the detrimental effect of Mn^{3+} on the rechargeable reaction.

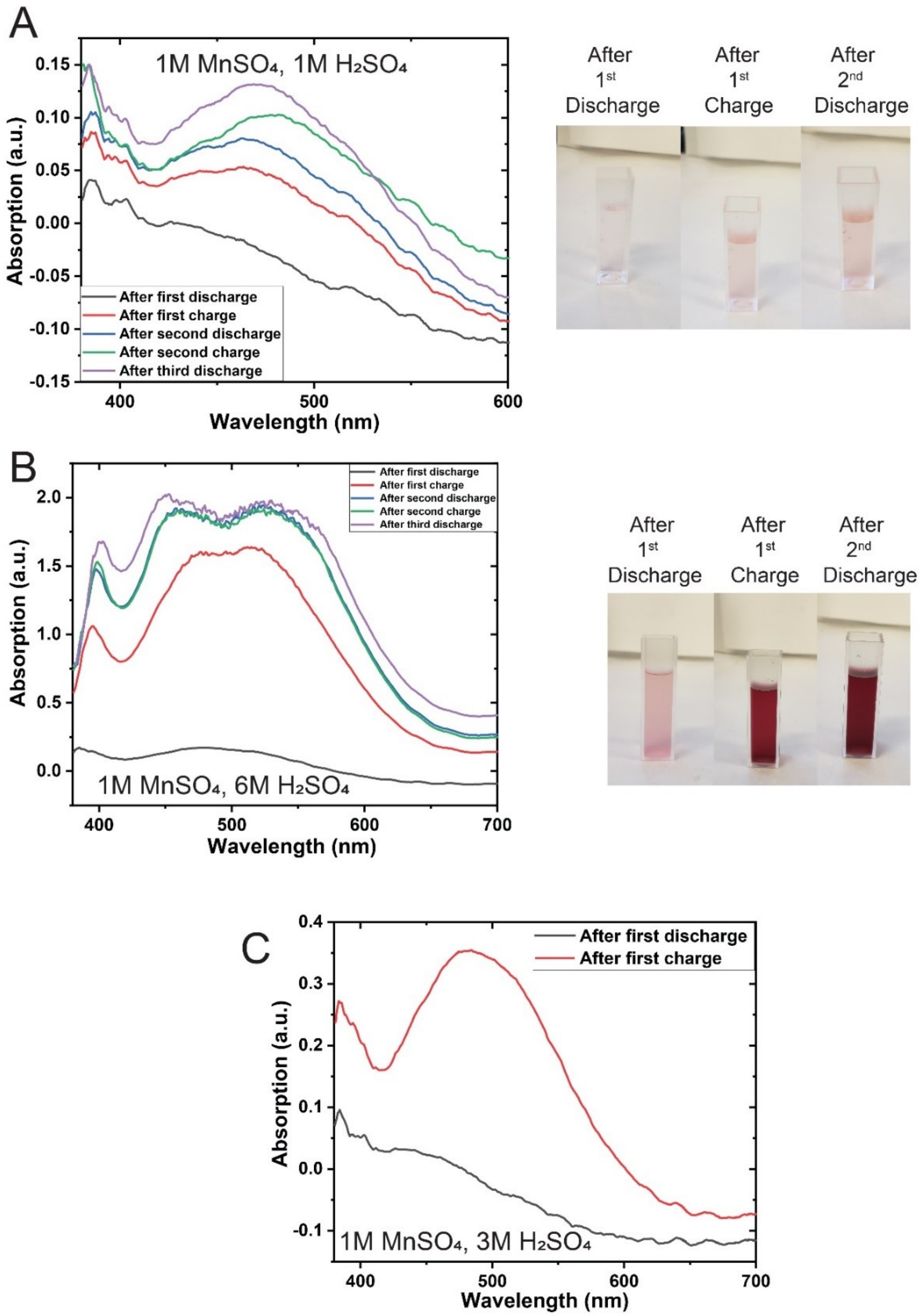

Supplementary Figure 3. UV-vis spectra of (A) a 1M $MnSO_4$ and 1M acid cycled catholyte with pictures of the solutions. (B) a 1M $MnSO_4$ and 6M acid cycled catholyte with pictures of the solutions showing deep red color formation (C) a 1M $MnSO_4$ and 3M acid cycled catholyte.

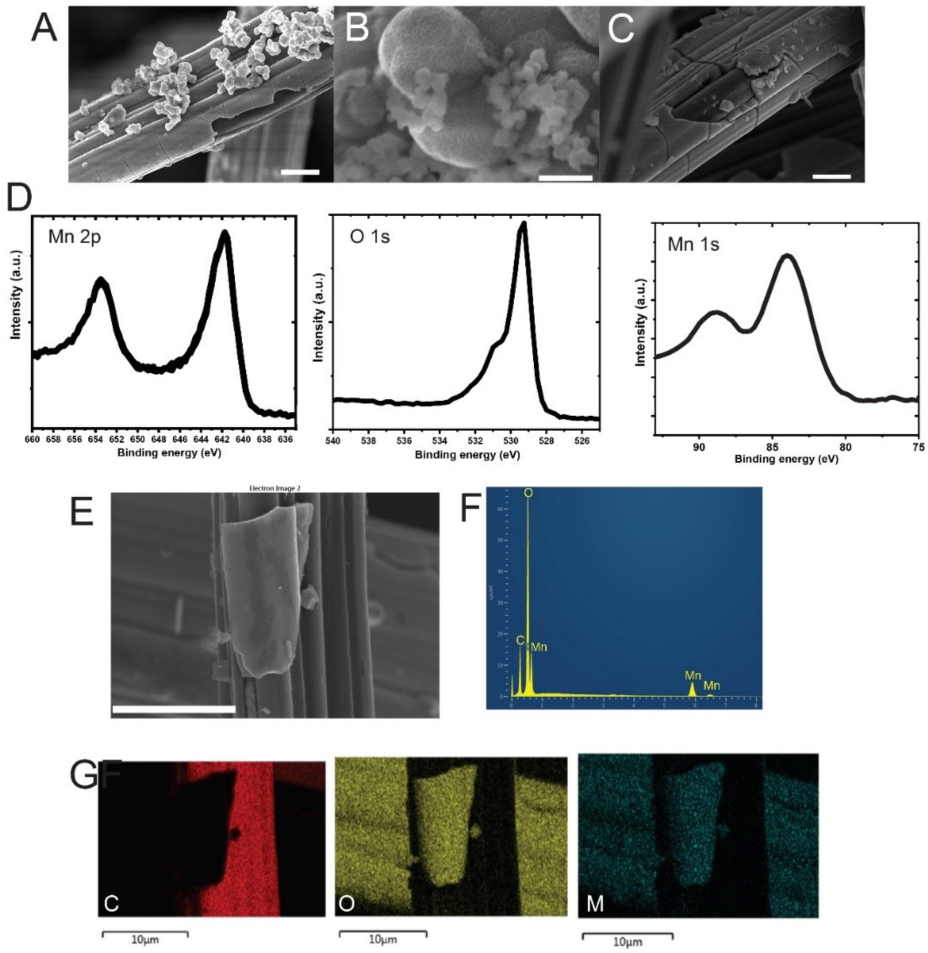

Supplementary Figure 4. (A) MnO_2 cathode cycled in 1M $MnSO_4$ and 1M acid catholyte (A) SEM image (scale bar is 5μm). (B) Magnified SEM image (scale bar is 500nm). (C) SEM image (scale bar is 5μm). (D) XPS spectra stopped on charge. (E) SEM image of cycled MnO_2 cathode (scale bar is 5um) where EDX was performed. (F) EDX spectra of cycled MnO_2 cathode shown in (E). (G) EDX elemental maps.

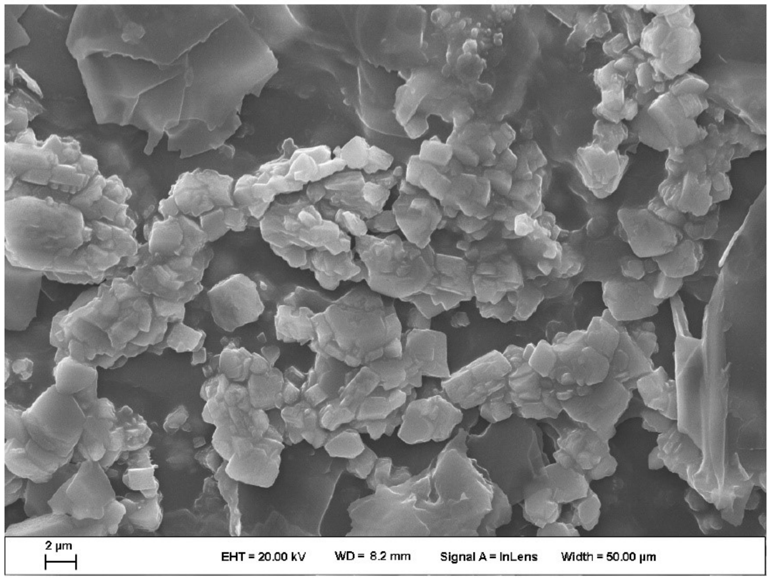

Supplementary Figure 5. SEM image of MnO_2 cathode cycled in 1M MnSO4 and 6M acid catholyte.

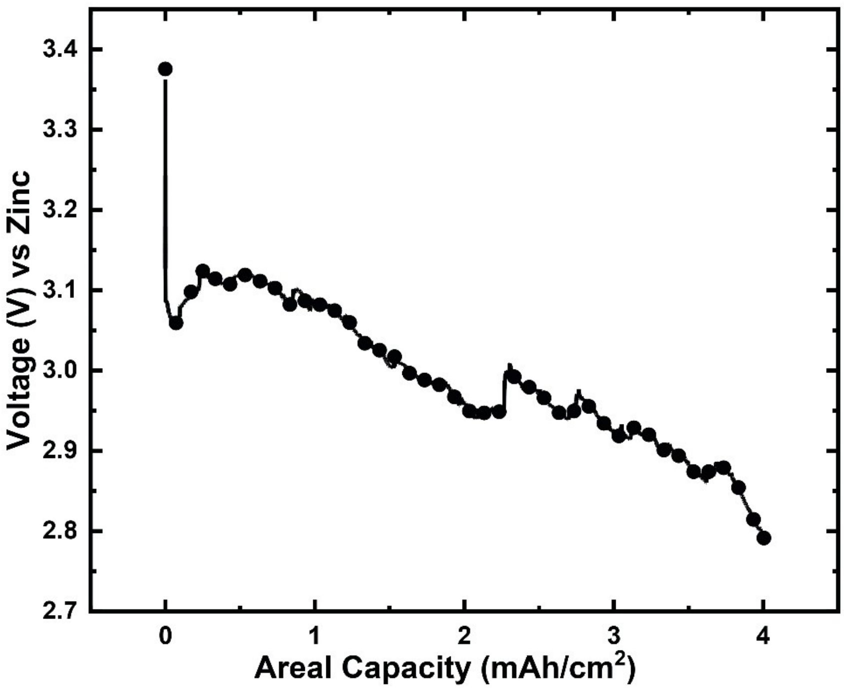

Supplementary Figure 6. Discharge curve of a high voltage Zn|MnO_2 with Nafion separator at 4mAh/cm^2 areal capacity. (10M H_2SO_4 catholyte and 50wt.% KOH anolyte)

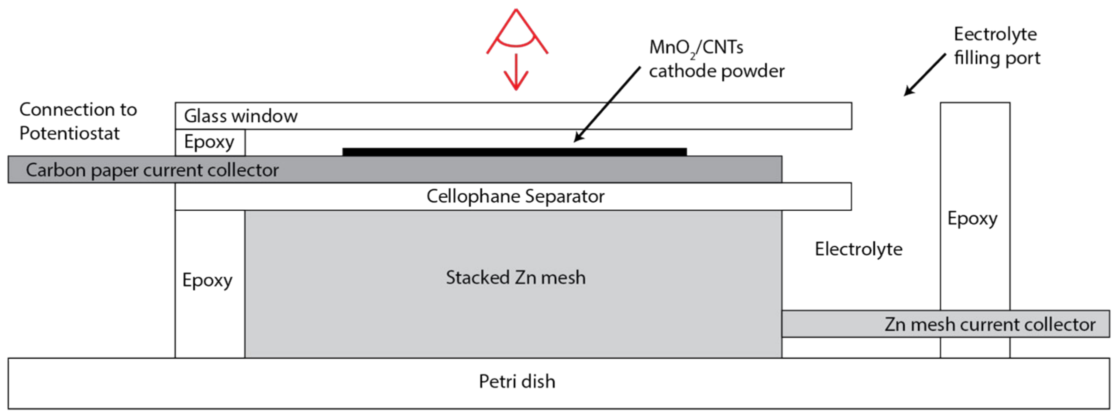

Supplementary Figure 7. Detailed schematic drawing of the microscopy cell used to capture in-situ reactions of MnO_2 and Zn in their respective electrolytes.

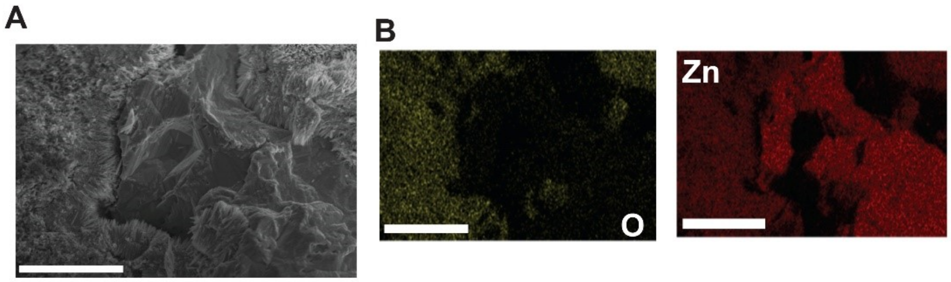

Supplementary Figure 8. (A) SEM image of cycled porous Zn anode in alkaline electrolyte where a Zn particle is covered by passivated ZnO shell (scale bar is 5um). (B) EDX elemental mapping of the SEM image shown in (A) where passivated ZnO shell is mapped (scale bar is 10µm).

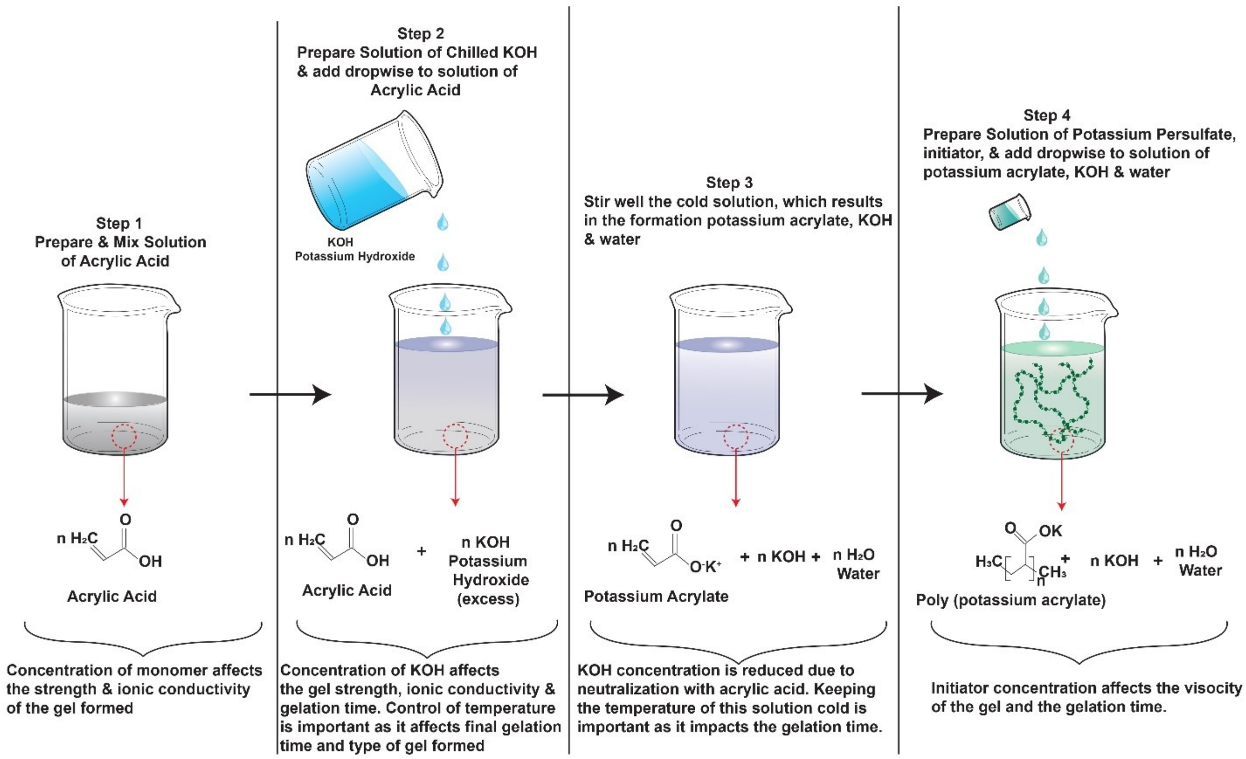

Supplementary Figure 9. Schematic drawing of the free radical polymerization method to synthesize alkaline polyacrylate and acid polyacrylic acid hydrogels. The buffer hydrogels were synthesized using the same method.

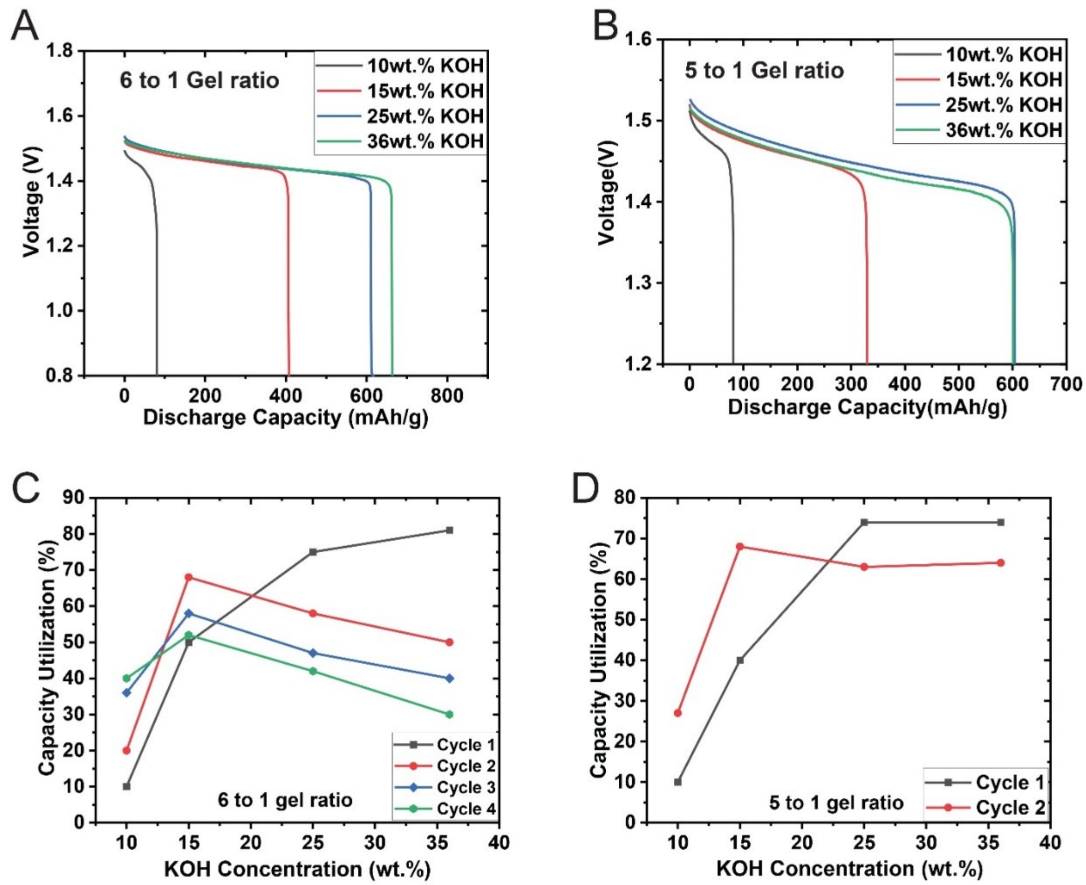

Supplementary Figure 10. Discharge curves of a (A) Zn mesh anode in 6 to 1 (KOH:acrylic acid) ratio in varying KOH hydrogel concentrations. (B) Zn mesh anode in 5 to 1 (KOH:acrylic acid) ratio in varying KOH hydrogel concentrations. Capacity utilization of a Zn mesh in varying KOH hydrogel concentrations in (C) 6:1 gel ratio for first four cycles (D) 5:1 gel ratio for first two cycles.

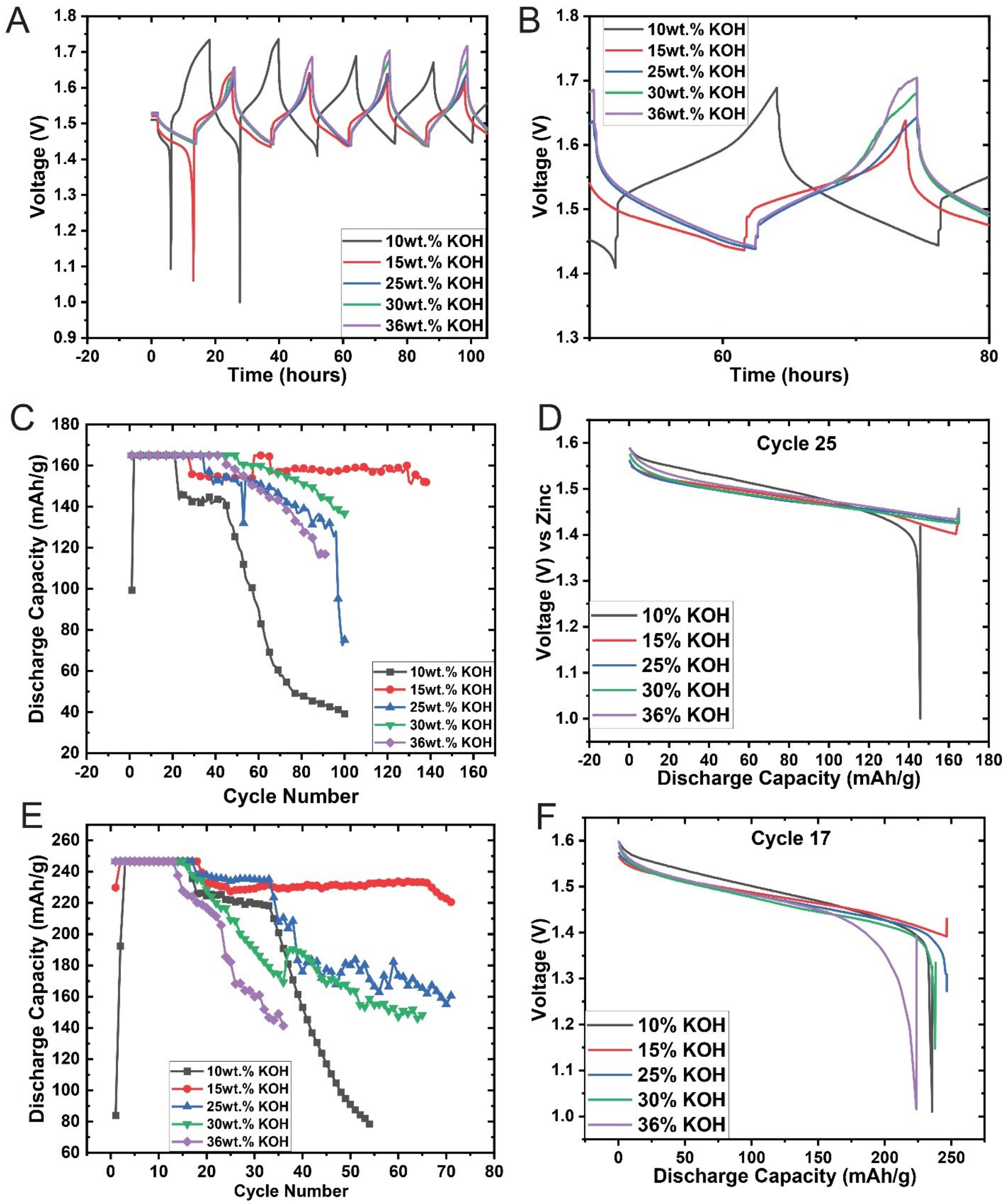

Supplementary Figure 11. (A) Cycling curves of Zn mesh at 20% utilization in varying KOH hydrogel concentrations. (B) Magnified cycling curves of Zn mesh in varying KOH hydrogel concentrations**.** (C) Capacity retention of Zn mesh at 20% utilization in varying KOH hydrogel concentrations**.** (D) Discharge capacity curve at cycle 25 of Zn mesh at 20% utilization in varying KOH hydrogel concentrations. (E) Capacity retention of Zn mesh at 30% utilization in varying

KOH hydrogel concentrations**.** (F) Discharge capacity curve at cycle 17 of Zn mesh at 30% utilization in varying KOH hydrogel concentrations.

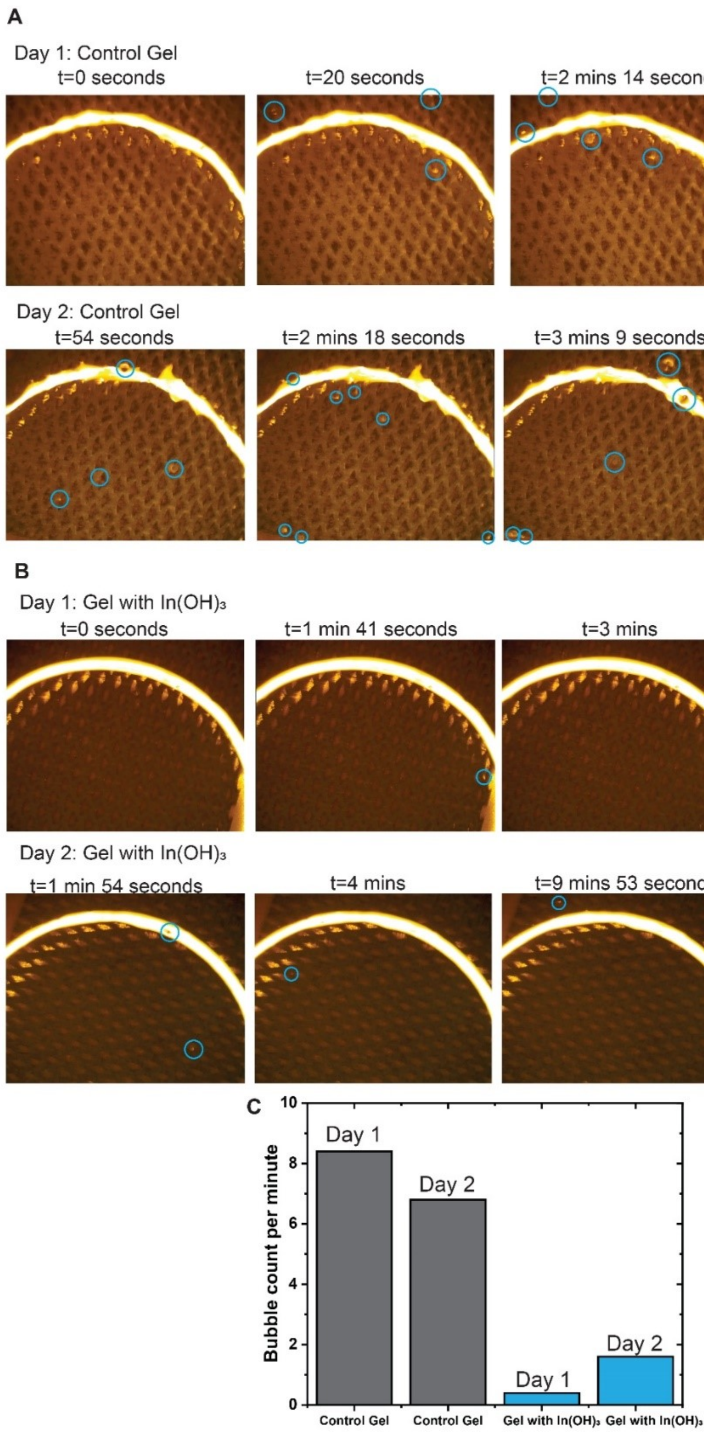
A
Day 1: Control Gel
t=0 seconds
t=20 seconds
t=2 mins 14 seconds
t=4 mins 44 seconds
Day 2: Control Gel
t=54 seconds
t=2 mins 18 seconds
t=3 mins 9 seconds
t=8 mins 47seconds
B
Day 1: Gel with In(OH)3
t=0 seconds
t=1 min 41 seconds
t=3 mins
t=5 mins
Day 2: Gel with In(OH)3
t=1 min 54 seconds
t=4 mins
t=9 mins 53 seconds
t=15 mins 8 seconds
C
Bubble count per minute
10
8
6
4
2
0
Day 1
Day 2
Day 1
Day 2
Control Gel
Control Gel
Gel with In(OH)3
Gel with In(OH)3

Supplementary Figure 12. (A) Microscope image capture of Zn mesh gas generation (as bubbles) in a poly(acrylate-KOH-MBA) hydrogel without indium hydroxide. (B) Microscope image capture of Zn mesh gas generation (as bubbles) in a poly(acrylate-KOH-MBA) hydrogel with indium hydroxide. (C) Bubble count per minute from microscope images of Zn mesh in hydrogels with and without indium hydroxide.

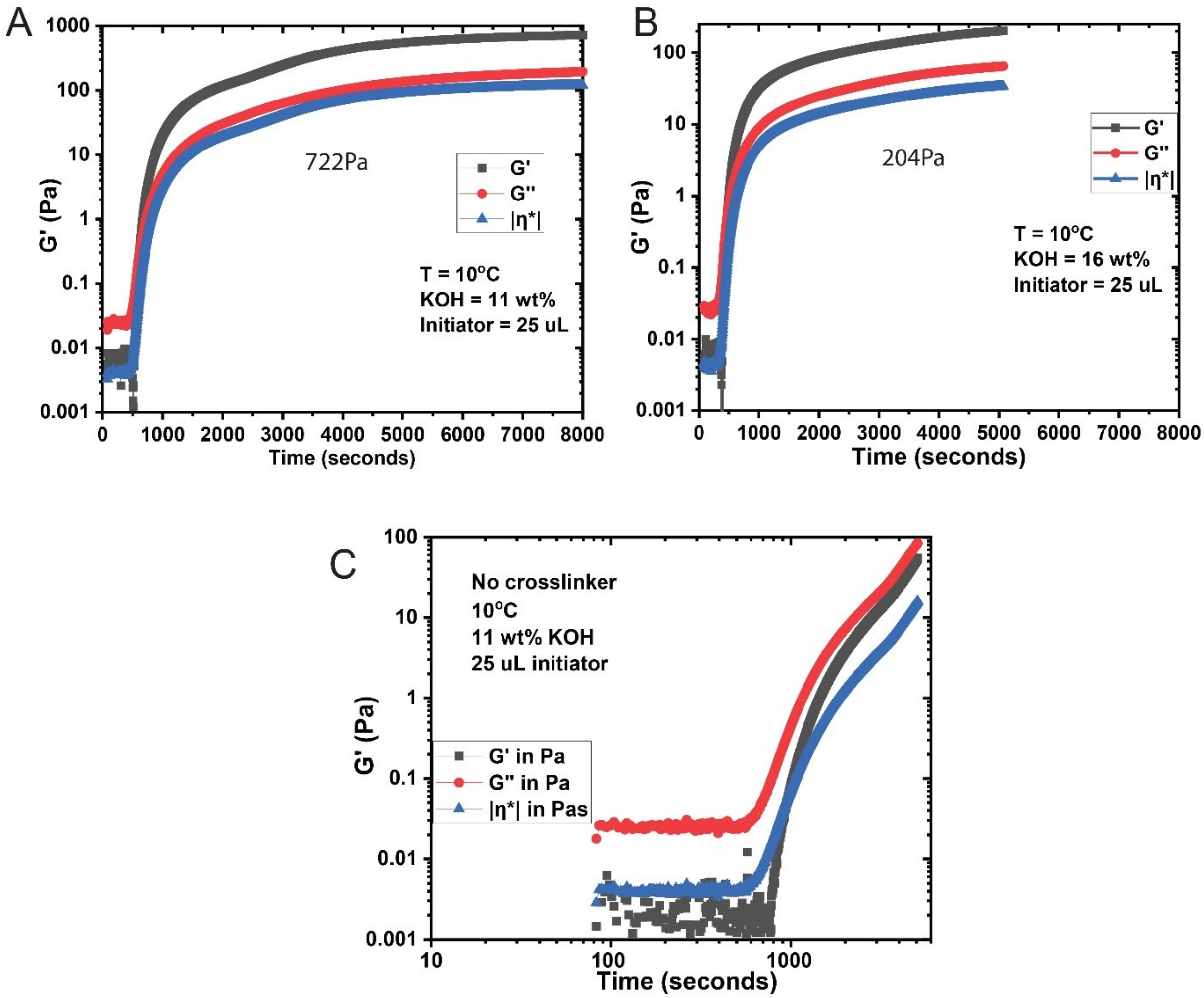

Supplementary Figure 13. Measurement of storage and loss modulus over time of (A) crosslinked 11wt.% KOH hydrogel. (B) crosslinked 16wt.% KOH hydrogel. (C) non-crosslinked 11wt.% KOH hydrogel.

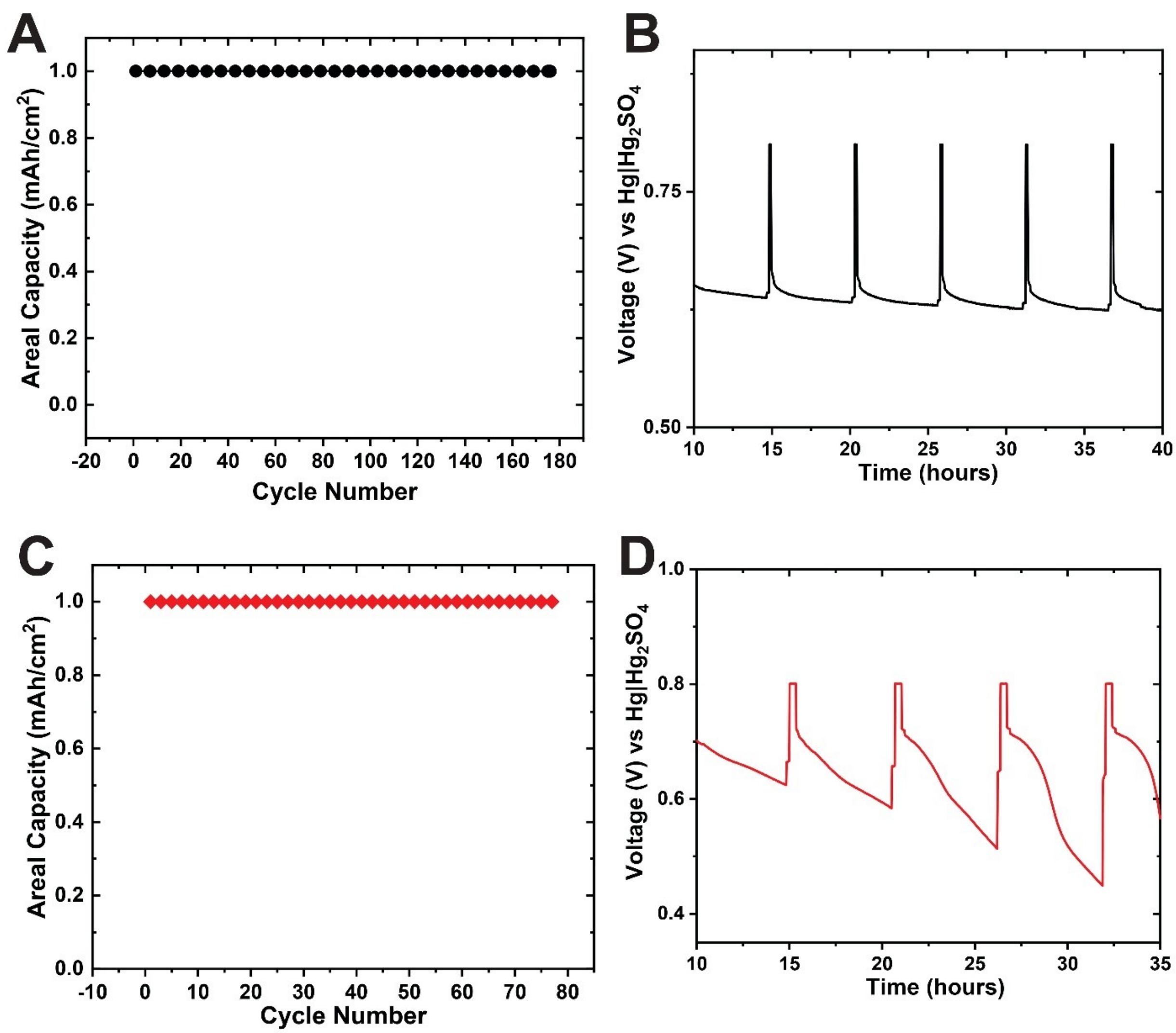

Supplementary Figure 14. (A) Areal capacity retention of MnO_2 cathode in 1M MnSO4 and 1M acid liquid catholyte. (B) Cycling curves of MnO_2 cathode in 1M MnSO4 and 1M acid liquid catholyte. (C) Areal capacity retention of MnO_2 cathode in 1M MnSO4 and 1M acid gelled catholyte. (D) Cycling curves of MnO_2 cathode in 1M MnSO4 and 1M acid gelled catholyte.

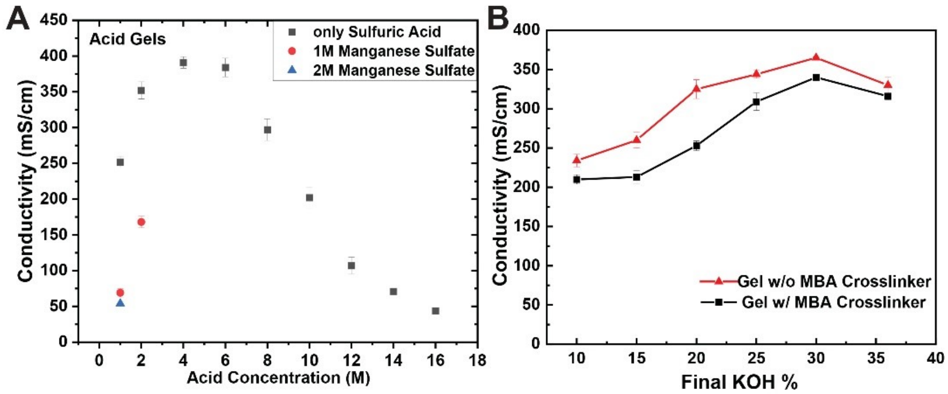

Supplementary Figure 15. (A) Ionic conductivity of crosslinked acid hydrogels. (B) Ionic conductivity of crosslinked and non-crosslinked alkaline hydrogels.

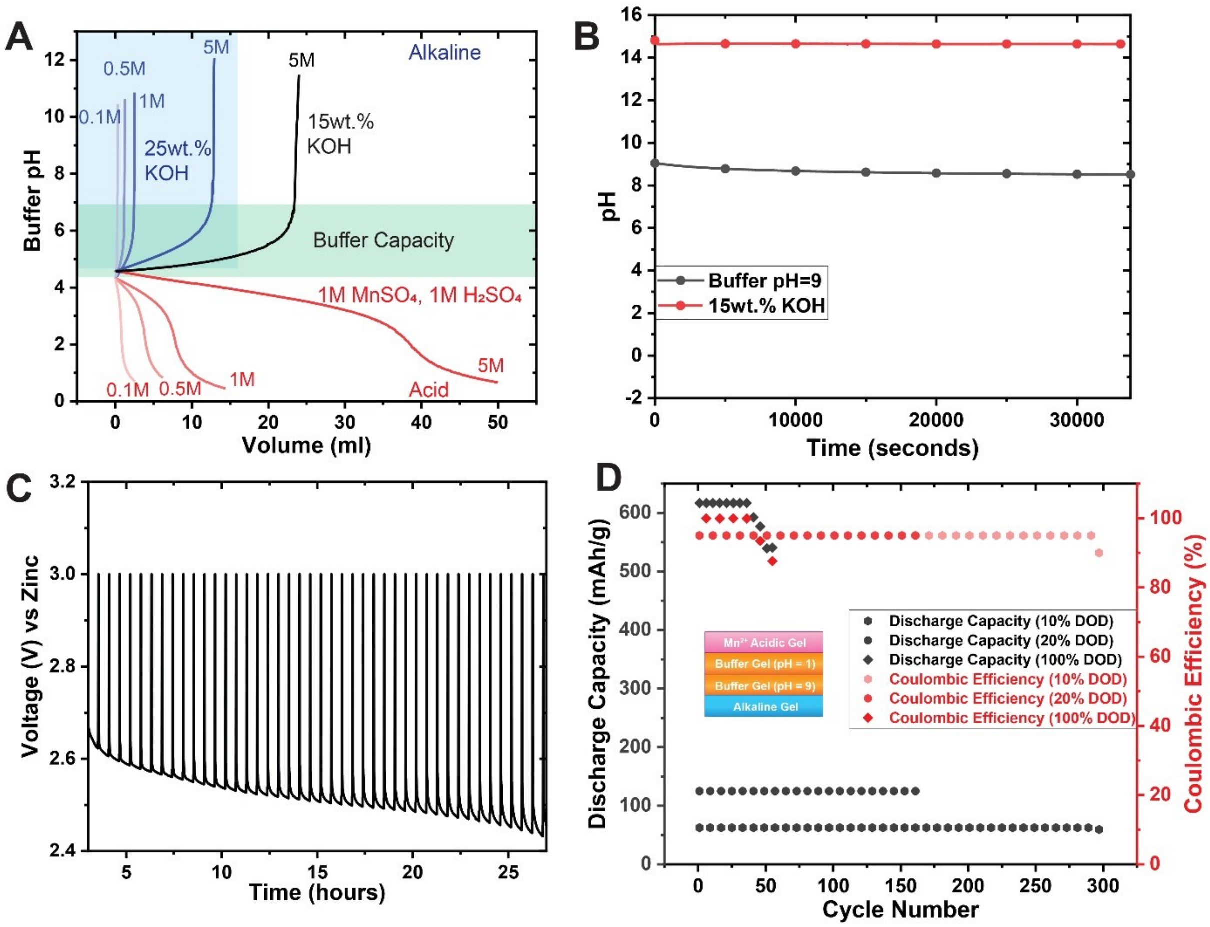

Supplementary Figure 16. (A) Measurement the buffering capacity of various concentrations of pH 5 buffer. (B) Real time pH measurement of alkaline and pH 9 buffer. (C) Cycling curves of a dual buffer layered (pH 1 and 9) membrane-less high voltage Zn|MnO_2 battery. (D) Capacity retention and coulombic efficiency of dual buffer layered(pH 1 and 9) membrane-less high voltage Zn|MnO_2 battery at 10%, 20% and 100% utilization of MnO_2's 2nd electron capacity.

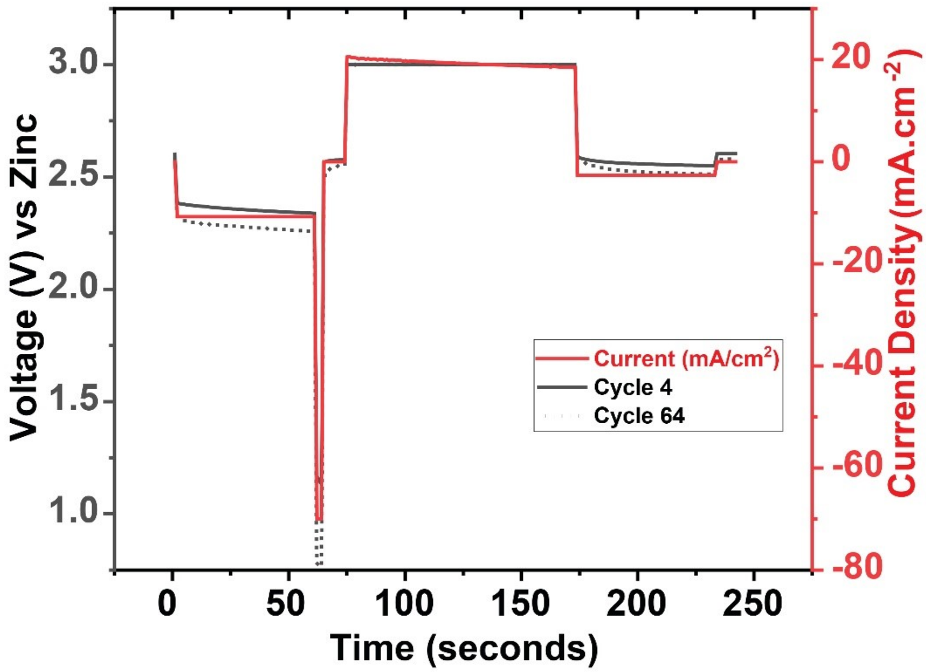

Supplementary Figure 17. Cycling of a high voltage Zn|MnO_2 battery following a BMW microhybrid protocol.